

MIT Open Access Articles

Analysis of the partial molar excess entropy of dilute hydrogen in liquid metals and its change at the solid-liquid transition

The MIT Faculty has made this article openly available. **Please share** how this access benefits you. Your story matters.

Citation: Caldwell, Andrew H. and Antoine Allanore. "Analysis of the partial molar excess entropy of dilute hydrogen in liquid metals and its change at the solid-liquid transition." Acta Materialia 173 (July 2019): 1-8.

As Published: <http://dx.doi.org/10.1016/j.actamat.2019.02.016>

Publisher: Elsevier BV

Persistent URL: <https://hdl.handle.net/1721.1/131149>

Version: Original manuscript: author's manuscript prior to formal peer review

Terms of use: Creative Commons Attribution-NonCommercial-NoDerivs License



Analysis of the Partial Molar Excess Entropy of Dilute Hydrogen in Liquid Metals and Its Change at the Solid-Liquid Transition

Andrew H. Caldwell^a, Antoine Allanore^{a,*}

^a*Department of Materials Science and Engineering, Massachusetts Institute of Technology,
77 Massachusetts Avenue, Cambridge, MA, 02139*

Abstract

A systematic change in the partial molar enthalpy of mixing ($\Delta\bar{h}_H^{\text{mix}}$) and partial molar excess entropy ($\Delta\bar{s}_H^{\text{ex}}$) for dilute hydrogen-metal systems at the solid-liquid transition is reported. Expressions for $\Delta\bar{h}_H^{\text{mix}}$ and $\Delta\bar{s}_H^{\text{ex}}$ are derived from the Fowler model of hydrogen solubility, and the change in $\Delta\bar{s}_H^{\text{ex}}$ at melting is bounded. The theoretical bound is in agreement with measured data. A connection is made between the change in $\Delta\bar{s}_H^{\text{ex}}$ and short range order in the metal-hydrogen system.

Keywords: Liquids, Hydrogen, Solubility, Statistical mechanics, Thermodynamics

1. Introduction

Metals processing invariably requires the handling of metals in the liquid state. Such operations rarely occur in inert atmospheres. The mole fraction of dissolved gases, in particular hydrogen (H), are typically in the range of 10^{-6} to 10^{-2} for liquid metals, and therefore degassing procedures are routinely employed in process metallurgy. This is done to prevent degradation of the mechanical properties of the solidified product, and such effects are well-studied [1, 2]. The severity of these effects depends on the concentration of H in the metal M, which can be determined from the solution thermodynamics of the M-H system. Calculating and predicting H solubility, defined here as its equilibrium

*Corresponding author

Email address: allanore@mit.edu (Antoine Allanore)

11 concentration in the metal, is therefore of considerable importance for metals
12 processing.

13 Prior reports have compiled existing data on the solubility of H in liquid
14 metals, along with dissolved oxygen, sulfur, and nitrogen [3, 4, 5]. These data
15 reveal a correlation between the two key quantities describing the mixing ther-
16 modynamics: the partial molar excess entropy ($\Delta\bar{s}_X^{\text{ex}}$) and the partial molar
17 enthalpy of mixing ($\Delta\bar{h}_X^{\text{mix}}$). $\Delta\bar{h}_X^{\text{mix}}$ is defined as

$$\Delta\bar{h}_X^{\text{mix}} = \bar{h}_X - \frac{1}{2}h_{X_2}^0 \quad (1)$$

18 where \bar{h}_X is the partial molar enthalpy, and $\frac{1}{2}h_{X_2}^0$ is the standard state enthalpy
19 of $X_{2(g)}$. $\Delta\bar{s}_X^{\text{ex}}$ is the defined as

$$\Delta\bar{s}_X^{\text{ex}} = \bar{s}_X - \frac{1}{2}s_{X_2}^0 - \bar{s}_X^{\text{id}} \quad (2)$$

20 where \bar{s}_X is the partial molar entropy, $s_{X_2}^0$ is the standard state entropy of $X_{2(g)}$,
21 and \bar{s}_X^{id} is the ideal partial molar entropy of mixing. The correlation between the
22 partial molar excess entropy ($\Delta\bar{s}_X^{\text{ex}}$) and the partial molar enthalpy of mixing
23 ($\Delta\bar{h}_X^{\text{mix}}$) for the liquid state can be rationalized from the chemical reactivity of
24 the metal-gas system, by considering the relative strength of the solute-metal
25 chemical bonding.

26 In the present work, specific attention is drawn to the solution behavior
27 of H in solid and liquid metals near T_{fus} and its statistical thermodynamic
28 description. Statistical thermodynamic treatments of H dissolved in a metal are
29 reported by a number of investigators[6, 7, 8, 9, 10, 11, 12, 13, 14, 15, 16, 17].
30 These studies derive $\Delta\bar{h}_H^{\text{mix}}$ and $\Delta\bar{s}_H^{\text{ex}}$ from the principles of statistical mechanics.
31 Together, these quantities define the activity coefficient (γ_H) as a function of
32 temperature and consequently the hydrogen concentration that is at equilibrium
33 with a given partial pressure of H_2 gas:

$$x_H = \frac{p_{H_2}^{\frac{1}{2}}}{\gamma_H} = p_{H_2}^{\frac{1}{2}} \exp \left[\frac{-\Delta\bar{h}_H^{\text{mix}}}{RT} + \frac{\Delta\bar{s}_H^{\text{ex}}}{R} \right]. \quad (3)$$

34 Eq. 3 is one form of what is referred to as Sieverts' law [18], which states that
35 the concentration of a gas solute X in a metal is proportional to the square-root
36 of the partial pressure of X_2 above the metal. Sieverts' law is valid in the dilute

limit and is generally observed for many M-H systems for $P_{\text{H}_2} \leq 1$ atm, in both the solid and liquid state. In Eq. 3, the proportionality constant is γ_{H} . In this analysis, γ_{H} , and by extension $\Delta \bar{h}_{\text{H}}^{\text{mix}}$ and $\Delta \bar{s}_{\text{H}}^{\text{ex}}$, are defined according to the following criteria:

1. The concentration coordinate for the system of a gas solute H in liquid metal M is the *mole fraction*, defined as $x_{\text{H}} \equiv n_{\text{H}}/(n_{\text{M}} + n_{\text{H}})$.
2. The standard state for the dissolved gas H is the *pure diatomic gas* $\frac{1}{2}\text{H}_2$ at 1 atm pressure.
3. The solution thermodynamics are treated in the limit of *infinite dilution*.

These criteria yield the definition shown in Eq. 3. The analysis presented herein restricts itself to the concentration and temperature regimes in which Eq. 3 is true¹. Thus, this analysis focuses on the *dilute* solution behavior of H in liquid metals, as this is the concentration regime most frequently encountered in metallurgical processes. “Dilute” here refers to concentrations for which H solute self-interaction is a negligible contribution to the H activity coefficient.

In this paper, we propose to compare H solubility data in liquid and solid metals near T_{fus} . Specifically, we report on a systematic shift in $\Delta \bar{h}_{\text{H}}^{\text{mix}}$ and $\Delta \bar{s}_{\text{H}}^{\text{ex}}$ at melting for a number of M-H systems. While not universal, the shift is sufficiently compelling as to suggest a common mechanism for the change in solution behavior that may be used to quantitatively predict the solution properties of H in liquid metals from solid-state data. A connection is made between the change in $\Delta \bar{s}_{\text{H}}^{\text{ex}}$ at melting and short range order in the liquid through a derivation of $\Delta \bar{h}_{\text{H}}^{\text{mix}}$ and $\Delta \bar{s}_{\text{H}}^{\text{ex}}$ from the proton gas model of Fowler and Smithells [6].

¹At approximately 2500 K (2227 °C) the equilibrium partial pressure of *monatomic* hydrogen gas $\text{H}_{(\text{g})}$ is on the order of a few percent and is therefore non-negligible. Above this temperature, H dissolution is no longer completely described by Eq. 3. Since the melting temperatures of the majority of elemental metals are less than 2500 K, Eq. 3 suffices for our discussion of the solution thermodynamics presented herein. Note, then, that for refractory metals (e.g., W, Mo) in the vicinity of T_{fus} there will necessarily be some error in the use of Eq. 3. For a perspective on $\text{H}_{(\text{g})}$ dissolution, see Gedeon and Eagar [19].

2. Change in $\Delta\bar{h}_H^{\text{mix}}$ and $\Delta\bar{s}_H^{\text{ex}}$ at the Solid-Liquid Transition

$\Delta\bar{h}_H^{\text{mix}}$ and $\Delta\bar{s}_H^{\text{ex}}$ are the change in the partial molar enthalpy of mixing and partial molar excess entropy, respectively. A partial molar property is the change in the integral property per addition of one atom of, for example, H to a liquid M-H solution. At the equilibrium solid-liquid transition we define the quantities $\Delta\Delta\bar{h}_H^{\text{mix}}$ and $\Delta\Delta\bar{s}_H^{\text{ex}}$:

$$\Delta\Delta\bar{h}_H^{\text{mix}} = \Delta\bar{h}_{H,\text{liq}}^{\text{mix}} - \Delta\bar{h}_{H,\text{sol}}^{\text{mix}} \quad (4)$$

$$\Delta\Delta\bar{s}_H^{\text{ex}} = \Delta\bar{s}_{H,\text{liq}}^{\text{ex}} - \Delta\bar{s}_{H,\text{sol}}^{\text{ex}} \quad (5)$$

The values of $\Delta\bar{h}_H^{\text{mix}}$ and $\Delta\bar{s}_H^{\text{ex}}$ for M-H systems for which solid- and liquid-state data exist are listed in Table 1. For each M-H system in Table 1 a quantity $T_{\text{sol}}/T_{\text{liq}}$ is defined to be the ratio of the maximum temperature for which the values $\Delta\bar{h}_{H,\text{sol}}^{\text{mix}}$ and $\Delta\bar{s}_{H,\text{sol}}^{\text{ex}}$ are valid to the minimum valid temperature for $\Delta\bar{h}_{H,\text{liq}}^{\text{mix}}$ and $\Delta\bar{s}_{H,\text{liq}}^{\text{ex}}$. For most of the M-H systems, $T_{\text{sol}}/T_{\text{liq}}$ is close to unity, indicating that $\Delta\Delta\bar{h}_H^{\text{mix}}$ and $\Delta\Delta\bar{s}_H^{\text{ex}}$ solely reflect changes in the solution behavior of dissolved H due to melting. It is important to recognize that, as a result of the weak temperature dependence of both $\Delta\bar{h}_H^{\text{mix}}$ and $\Delta\bar{s}_H^{\text{ex}}$ [20], the temperature range over which reported values of these properties quantitatively describe the solution behavior is usually several hundreds of degrees Celsius. Thus, it is reasonable to treat $\Delta\Delta\bar{h}_H^{\text{mix}}$ and $\Delta\Delta\bar{s}_H^{\text{ex}}$ as capturing the change in $\Delta\bar{h}_H^{\text{mix}}$ and $\Delta\bar{s}_H^{\text{ex}}$ across the solid-liquid transition for systems with $T_{\text{sol}}/T_{\text{liq}}$ close to unity. For systems with $T_{\text{sol}}/T_{\text{liq}}$ far from unity, there is greater uncertainty with this assumption.

Table 1: Values of $\Delta\bar{h}_H^{\text{mix}}$ and $\Delta\bar{s}_H^{\text{ex}}$ for H in elemental metals

System	$\Delta\bar{h}_H^{\text{mix}}$ kJ (mol H) ⁻¹	$\Delta\bar{s}_H^{\text{ex}}$ J K ⁻¹ (mol H) ⁻¹	$T_{\text{sol}}/T_{\text{liq}}$	References
Ag _(l)	76.3	-29.5		[21]
Ag _(s)	62.1	-48.5	0.98	[21]
Ag _(s) ⁽²⁾	68.9	-42.5	1.0	[22], see also: [4]

Continued on next page

System	$\Delta \bar{h}_{\text{H}}^{\text{mix}}$ kJ (mol H) ⁻¹	$\Delta \bar{s}_{\text{H}}^{\text{ex}}$ J K ⁻¹ (mol H) ⁻¹	$T_{\text{sol}}/T_{\text{liq}}$	References
Al _(l)	51.5	-36.2		[23]
Al _(s)	58.2	-56.7	1.0	[23]
Al _(s) ⁽²⁾	56.8	-54.0	1.0	[24]
Co _(l)	41.0	-33.9		[4], see also: [25]
Co _(s)	32.2	-45.7	1.0	[4]
Cu _(l)	43.5	-35.3		[26], [25]
Cu _(s)	34.5	-46.2	0.94	[26]
Cu _(s) ⁽²⁾	49.0	-41.0	1.0	[22]
Fe _(l)	36.4	-35.3		[25]
Fe _α	22.2	-53.6	0.65	[26], see also: [27]
Fe _α ⁽²⁾	24.3	-53.6	0.65	[22], see also: [27]
Fe _γ	27.0	-46.7	0.92	[26], see also: [27]
Fe _γ ⁽²⁾	29.9	-45.6	0.92	[22], see also: [27]
Fe _δ	28.8	-46.4	1.0	[22], see also: [27]
Mg _(l)	29.6	-26.2		[28]
Mg _(s)	19.3	-40.4	0.70	[28]
Mn _(l)	24.9	-32.4		[29]
Mn _α	11.3	-46.9	0.65	[30]
Mn _δ	13.4	-42.5	1.0	[30]
Nb _(l)	-31.0	-47.3		[4]
Nb _(s)	-36.1	-49.6	0.18	[31]
Nb _(s) ⁽²⁾	-39.6	-65.3	0.18	[22]
Nb _(s) ⁽³⁾	-35.3	-58.0	0.37	[32]
Ni _(l)	20.0	-39.7		[25]
Ni _(s)	16.6	-48.7	0.88	[33]
Pd _(l)	-16.4	-48.2		[34]
Pd _(s)	-14.1	-53.8	0.99	[34]
Pd _(s) ⁽²⁾	-10.3	-51.3	0.19	[22]
Ti _(l)	-41.1	-44.5		[35]
Ti _(s)	-40.2	-43.3	0.38	[36]
Ti _(s) ⁽²⁾	-59.8	-49.9	0.71	[20]

Continued on next page

System	$\Delta\bar{h}_H^{\text{mix}}$ kJ (mol H) ⁻¹	$\Delta\bar{s}_H^{\text{ex}}$ J K ⁻¹ (mol H) ⁻¹	$T_{\text{sol}}/T_{\text{liq}}$	References
U _(l)	11.2	-33.7		[4]
U _(s)	43.4	-42.9	1.0	[4]

81 The data in Table 1 are plotted in Fig. 1 where $\Delta\Delta\bar{h}_H^{\text{mix}}R^{-1}$ is the ordinate
 82 and $\Delta\Delta\bar{s}_H^{\text{ex}}R^{-1}$ is the abscissa (R is the gas constant). The data point labels
 83 indicate the solid phase of the metal considered in the calculation of $\Delta\Delta\bar{h}_H^{\text{mix}}$
 84 and $\Delta\Delta\bar{s}_H^{\text{ex}}$. For example, “Fe_α” refers to the alpha phase of Fe. The superscript
 85 numbers distinguish multiple values of $\Delta\bar{h}_H^{\text{mix}}$ and $\Delta\bar{s}_H^{\text{ex}}$ reported for the solid
 86 phase. A single set of values is used for the liquid phase data for each M-H
 87 system.

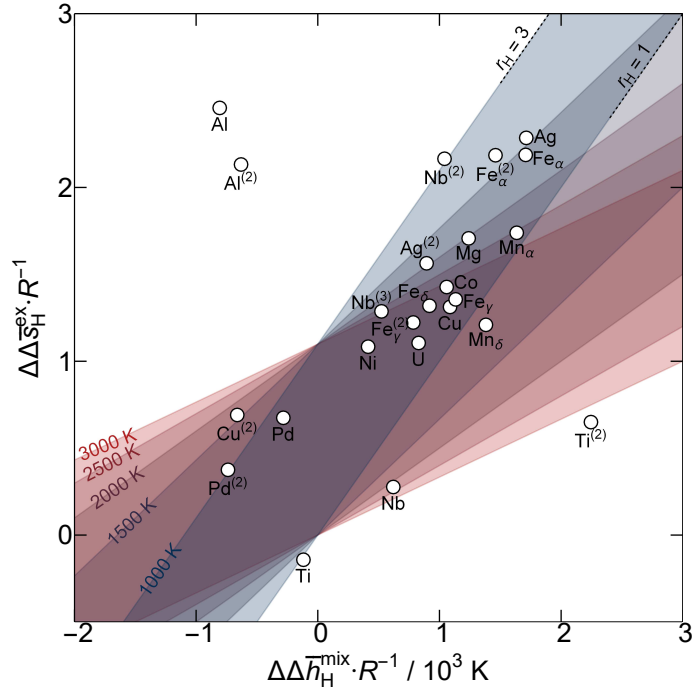


Figure 1: Partial molar excess entropy ($\Delta\Delta\bar{s}_H^{\text{ex}}$, see Eq. 5) variation at melt-
 ing versus the corresponding variation in the partial molar enthalpy of mixing
 ($\Delta\Delta\bar{h}_H^{\text{mix}}$, see Eq. 4) for M-H systems. Point labels denote the solid phase consid-
 ered in the calculation of $\Delta\Delta\bar{h}_H^{\text{mix}}$ and $\Delta\Delta\bar{s}_H^{\text{ex}}$. The shaded regions are contours,
 at different temperatures, of the surface defined by $1 \leq r_H \equiv (x_{\text{H,liq}}/x_{\text{H,sol}}) \leq 3$
 (see Eq. 6).

Together, $\Delta\Delta\bar{h}_H^{\text{mix}}$ and $\Delta\Delta\bar{s}_H^{\text{ex}}$ reflect changes in the equilibrium mole fraction of dissolved H. From Eqs. 3, 4, and 5, and for a constant p_{H_2} , we define the liquid-to-solid H solubility ratio, r_H , as

$$r_H = \frac{x_{\text{H,liq}}}{x_{\text{H,sol}}} = \exp \left[\frac{-\Delta\Delta\bar{h}_H^{\text{mix}}}{RT_{\text{fus}}} + \frac{\Delta\Delta\bar{s}_H^{\text{ex}}}{R} \right]. \quad (6)$$

A plot of $\Delta\Delta\bar{s}_H^{\text{ex}}$ versus $\Delta\Delta\bar{h}_H^{\text{mix}}$ therefore defines a surface of the change in equilibrium H solubility for a given temperature. In Fig. 1 the shaded regions are contours of this surface. Each contour defines the inequality $1 \leq r_H \leq 3$ at a specific value of T_{fus} . Five contours are shown, from 1000 K (727 °C) to 3000 K (2727 °C) in steps of 500 K. This range of temperatures bounds T_{fus} for the majority of metals.

Most of the data in Fig. 1 lie within the contours of the 1-to-3 times increase in solubility over the T_{fus} range of 1000–3000 K. This observation reflects the consensus in metallurgy that H solubility increases slightly upon melting [5]. Furthermore, it is clear that the distribution of $\Delta\Delta\bar{h}_H^{\text{mix}}$ and $\Delta\Delta\bar{s}_H^{\text{ex}}$ is non-random. Values of $\Delta\Delta\bar{h}_H^{\text{mix}}$ and $\Delta\Delta\bar{s}_H^{\text{ex}}$ are within $0\text{--}2000R$ ($\text{J mol}^{-1} \text{ H}$) and $0\text{--}2R$ ($\text{J K}^{-1} \text{ mol}^{-1} \text{ H}$), respectively. There is a clustering of the data at approximately $1000R$ for $\Delta\Delta\bar{h}_H^{\text{mix}}$ and $1.3R$ for $\Delta\Delta\bar{s}_H^{\text{ex}}$. The fact that chemically-dissimilar metals, such as Fe, Ag, U, and Nb, exhibit similar values of $\Delta\Delta\bar{h}_H^{\text{mix}}$ and $\Delta\Delta\bar{s}_H^{\text{ex}}$, in the vicinity of $1000R$ and $1.3R$, respectively, suggests that a common mechanism is responsible for the change in solution behavior of H across melting. We later adopt $\Delta\Delta\bar{h}_H^{\text{mix}} = 1000R$ and $\Delta\Delta\bar{s}_H^{\text{ex}} = 1.3R$ as characteristic values.

The characteristic values of $\Delta\Delta\bar{h}_H^{\text{mix}}$ and $\Delta\Delta\bar{s}_H^{\text{ex}}$ may not be universally applicable. As Fig. 1 illustrates, outliers such as the Al-H system exist. In addition, uncertainties in the values of reported partial molar mixing quantities, like $\Delta\bar{h}_H^{\text{mix}}$ and $\Delta\bar{s}_H^{\text{ex}}$, tend to be large [37], and so drawing more precise correlations from the $\Delta\Delta\bar{h}_H^{\text{mix}}$ and $\Delta\Delta\bar{s}_H^{\text{ex}}$ data should be done with some caution. In the absence of reported experimental uncertainties for $\Delta\bar{h}_H^{\text{mix}}$ and $\Delta\bar{s}_H^{\text{ex}}$, recourse should be made to reported uncertainties for other liquid metal-gas systems (e.g., M-O) and to liquid metal alloys in general to guide our understanding of the degree of scatter in the data shown in Fig. 1. Partial molar excess entropies and enthalpies of mixing are known to within about $1 \text{ J mol}^{-1} \text{ K}^{-1}$ and

119 1 kJ mol⁻¹, respectively [3, 38]. An approximate uncertainty for the data points
 120 in Fig. 1 may then be represented by error bars of ± 0.2 . This uncertainty does
 121 not change the systematic trend illustrated in Fig. 1.

122 Nevertheless, a characteristic change in $\Delta\bar{h}_H^{\text{mix}}$ and $\Delta\bar{s}_H^{\text{ex}}$ across melting may
 123 not be entirely surprising. Among the gas solutes frequently encountered in
 124 metallurgy—H, O, S, and N—hydrogen is the least reactive, with the smallest
 125 electronegativity difference. Dissolved H, particularly at high temperatures in
 126 the dilute regime (where the number of available H sites is much greater than the
 127 number of H atoms), is therefore more “gas-like” than, for example, dissolved
 128 O. It may be surmised, then, that changes in the quantities that define the
 129 interaction between M and H, i.e., $\Delta\bar{h}_H^{\text{mix}}$ and $\Delta\bar{s}_H^{\text{ex}}$, due to melting are the result
 130 of *structural* changes in the metal itself, more so than the result of changes in
 131 the specific chemical interaction. “Structural” here entails properties such as
 132 coordination number, molar volume, and ordering. Since the structural changes
 133 that occur during melting of most crystalline metals are often considered similar
 134 (see, for example, similarities in the entropies of fusion [39]), it can be argued
 135 that $\Delta\Delta\bar{h}_H^{\text{mix}}$ and $\Delta\Delta\bar{s}_H^{\text{ex}}$ should be similar as well for different M-H systems.

136 3. Derivation of $\Delta\Delta\bar{h}_H^{\text{mix}}$ and $\Delta\Delta\bar{s}_H^{\text{ex}}$ from a Statistical Model of H 137 Solubility

138 In the previous section it was found that the change in $\Delta\bar{h}_H^{\text{mix}}$ and $\Delta\bar{s}_H^{\text{ex}}$ at the
 139 solid-liquid transition is around $1000R$ and $1.3R$, respectively, for most of the
 140 M-H systems in Table 1, constituting a characteristic shift in the equilibrium
 141 H concentration. A rationalization for the magnitude of these quantities is
 142 provided in the following using the statistical mechanical model of H solubility
 143 proposed by Fowler and Smithells [6]. This is the “proton gas” model, in which
 144 the metal, either solid or liquid, is treated as a potential field through which H
 145 atoms move.

146 The grand canonical partition function (Γ) of dissolved H in a metal M of
 147 volume V may be written as :

$$\Gamma = \exp \left(l_H \lambda_H \omega e^{-\chi_s/kT} \right). \quad (7)$$

148 The derivation of this form of Γ is given in Appendix A. l_H (Eq. 8) is the
 149 molecular translational partition function, λ_H is the absolute activity of H, ω is
 150 the H nuclear spin statistical weight, and χ_s is the ground state energy of H in
 151 the metal, referenced to the state of infinite separation outside the metal.

$$l_H = \left(\frac{2\pi m_H kT}{h^2} \right)^{3/2} V_H \quad (8)$$

152 In Eq. 8, V_H (Eq. 9) may be thought of as the effective volume in the metal over
 153 which H atoms behave “gas-like”. It is the classical configuration integral.² V_H
 154 is critical for connecting $\Delta\bar{s}_H^{\text{ex}}$ to short range ordering.

$$V_H = \int_V e^{-W/kT} dV \quad (9)$$

155 In Eq. 9, W is the configurational potential energy of the H assembly referenced
 156 to the lowest energy state of H in the metal and is a function of the positional
 157 coordinates of the H atoms.

158 The equilibrium number of dissolved H, N_H , is

$$N_H = kT \left(\frac{\partial \ln \Gamma}{\partial \mu_H} \right) = l_H \lambda_H \omega e^{-\chi_s/kT} \quad (10)$$

159 The derivation of $\Delta\bar{s}_H^{\text{ex}}$ follows from the definition of the partial molar en-
 160 tropy as the temperature-derivative of the chemical potential. It is convenient
 161 to first convert the number of H atoms into the atomic ratio³ of H atoms and
 162 M atoms, as shown in Eq. 11.

$$\frac{N_H}{N_M} = \frac{l_H}{V} \lambda_H \omega \frac{M_M}{\rho_M N_A} e^{-\chi_s/kT} \quad (11)$$

163 The chemical potential of dissolved H may then be written as:

$$\mu_H = kT \ln \lambda_H = kT \ln \left(\frac{N_H}{N_M} \theta(T) \right) \quad (12)$$

²The quantity $V_H^{N_H}/N_H!$ is sometimes referred to as the configurational potential energy partition function [40].

³In the limit of infinite dilution, the atomic ratio is equivalent to the atomic fraction, and so this conversion introduces no error with regards to the experimental data, which is defined with respect to atomic fraction.

164 where $\theta(T) = \left(\frac{l_H}{V} \omega \frac{M_M}{\rho_M N_A} e^{-\chi_s/kT} \right)^{-1}$. Taking the derivative of μ_H with respect
 165 to temperature at constant P and N_H , the total partial molar entropy is:

$$\bar{s}_H = -k \ln \left(\frac{N_H}{N_M} \right) - k \left(T \frac{\partial \ln \theta(T)}{\partial T} + \ln \theta(T) \right). \quad (13)$$

166 The ideal configurational component is $-k \ln (N_H/N_M)$. Substituting for $\theta(T)$,
 167 one finds for the excess component:

$$\frac{\bar{s}_H^{\text{ex}}}{k} = \frac{3}{2} + \frac{1}{kT} \frac{\partial \ln V_H}{\partial T} + \frac{3}{2} \ln \left(\frac{2\pi m_H kT}{h^2} \right) + \ln \left(\frac{V_H}{V} \right) + \ln \omega + \ln \left(\frac{M_M}{\rho_M N_A} \right) \quad (14)$$

168 As discussed in the Introduction, the chosen standard state of dissolved H is
 169 the $\frac{1}{2}\text{H}_2$ gas standard state. The “relative” partial molar excess entropy, $\Delta \bar{s}_H^{\text{ex}}$,
 170 is then $\bar{s}_H^{\text{ex}} - \frac{1}{2} s_{\text{H}_2}^0$. Upon subtracting the entropy of H gas (see Appendix B),
 171 one finds:

$$\frac{\Delta \bar{s}_H^{\text{ex}}}{k} = \frac{1}{4} \left(\ln \left(\frac{m_H^3}{16\pi A^2 k h^2 T} \right) - 1 \right) + \ln \left(\frac{M_M}{\rho_M N_A} \right) + \frac{1}{2} \ln P + \ln \left(\frac{V_H}{V} \right) + \frac{1}{kT} \frac{\partial \ln V_H}{\partial T} \quad (15)$$

172 The relative partial molar enthalpy, $\Delta \bar{h}_H^{\text{mix}}$, can be derived following the
 173 same steps taken for Eqs. 13–15, where instead the Gibbs-Helmholtz relation
 174 defines the enthalpy from the chemical potential. For concision, we omit these
 175 steps and present the expression for $\Delta \bar{h}_H^{\text{mix}}$ in Eq. 16.

$$\frac{\Delta \bar{h}_H^{\text{mix}}}{kT} = \frac{\chi_s + \frac{1}{2}\chi_d}{kT} - \frac{1}{4} + \frac{1}{kT} \frac{\partial \ln V_H}{\partial T} \quad (16)$$

176 It is important to note here that the terms in the expressions for $\Delta \bar{h}_H^{\text{mix}}/kT$
 177 (Eq. 15) and $\Delta \bar{s}_H^{\text{ex}}/k$ (Eq. 16) that are of the same order in T cannot be dis-
 178 tinguished as “enthalpic” or “entropic” if, experimentally, $\Delta \bar{h}_H^{\text{mix}}$ and $\Delta \bar{s}_H^{\text{ex}}$ are
 179 calculated from an Arrhenius fitting of temperature-composition data. Conse-
 180 quently, it is prudent to define “effective” values of $\Delta \bar{h}_H^{\text{mix}}$ and $\Delta \bar{s}_H^{\text{ex}}$ that are the
 181 result of allowing like-terms in the quantities $\Delta \bar{h}_H^{\text{mix}}/kT$ and $\Delta \bar{s}_H^{\text{ex}}/k$ to com-
 182 bine. The effective values of $\Delta \bar{h}_H^{\text{mix}}$ and $\Delta \bar{s}_H^{\text{ex}}$ may then be identified directly
 183 from Eq. 3. In doing so, a valid comparison can be made between the theoretical
 184 and measured values of $\Delta \bar{h}_H^{\text{mix}}$ and $\Delta \bar{s}_H^{\text{ex}}$. Eqs. 17 and 18 define the effective
 185 values of $\Delta \bar{h}_H^{\text{mix}}$ and $\Delta \bar{s}_H^{\text{ex}}$, respectively, in the proton gas model. For clarity, we
 186 will continue to refer to these quantities as $\Delta \bar{h}_H^{\text{mix}}$ and $\Delta \bar{s}_H^{\text{ex}}$.

$$\frac{\Delta \bar{h}_H^{\text{mix}}}{kT} = \frac{\chi_s + \frac{1}{2}\chi_d}{kT} \quad (17)$$

$$\frac{\Delta \bar{s}_H^{\text{ex}}}{k} = \frac{1}{4} \ln \left(\frac{m_H^3}{16\pi A^2 k h^2 T} \right) + \ln \left(\frac{M_M}{\rho_M N_A} \right) + \frac{1}{2} \ln P + \ln \left(\frac{V_H}{V} \right) \quad (18)$$

At this point, it is valuable to compare these results with experimental data. Fig. 2 is a plot of reported values of $\Delta \bar{s}_X^{\text{ex}}/R$ versus $1/T$ for M-X systems, where X is H, O, S, or N. The data point labels indicate the elemental *liquid* metal, M. The temperature coordinate of each data point is the lower bound of the temperature range for which the measured solution property, here $\Delta \bar{s}_X^{\text{ex}}$, is valid. For most of the M-X systems shown in Fig. 2 this temperature is in the vicinity of T_{fus} , though obvious exceptions exist (e.g., Al-O). Of primary interest here is the shaded band, which is the theoretical $\Delta \bar{s}_H^{\text{ex}}$ (Eq. 18) for values of V_H/V between 0.1 (lower curve) and 1.0 (upper curve). The density (ρ_M) and molar mass (M_M) are 10^4 kg m^{-3} and 0.1 kg mol^{-1} , respectively, chosen as representative values for the elemental liquid metals.

The measured values of $\Delta \bar{s}_H^{\text{ex}}$ are well-described by the results of the proton gas model within the bounds of $0.1 \leq V_H/V \leq 1.0$. This corroborates a similar observation by Fowler and Guggenheim for solid transition metal-hydrogen systems in the dilute limit [40]. Given that the majority of the M-H systems in Fig. 2 fall within $0.1 \leq V_H/V \leq 1.0$, one may argue that values of $\Delta \bar{s}_H^{\text{ex}}$ well outside this range are suspect. The status of Au-H and Cr-H as outliers is therefore likely due to experimental uncertainty.

A comparison may also be made with the entropy of the gas phase. The solid curves in Fig. 2 show $\frac{1}{2}s_{X_2}^0$ as a function of temperature. If $\Delta \bar{s}_H^{\text{ex}}$ is taken to be its average value near $-4.5R$, the difference between $\Delta \bar{s}_H^{\text{ex}}$ and $\frac{1}{2}s_{X_2}^0$ is about $5R$ to $8R$. This represents the excess entropy arising from solute-solvent interaction.

4. Discussion

4.1. $\Delta \bar{s}_H^{\text{ex}}$ and Short Range Order

The quantity V_H (Eq. 9) in the proton gas model can be treated as a fitting parameter for interpreting experimentally measured values of $\Delta \bar{s}_H^{\text{ex}}$. However,

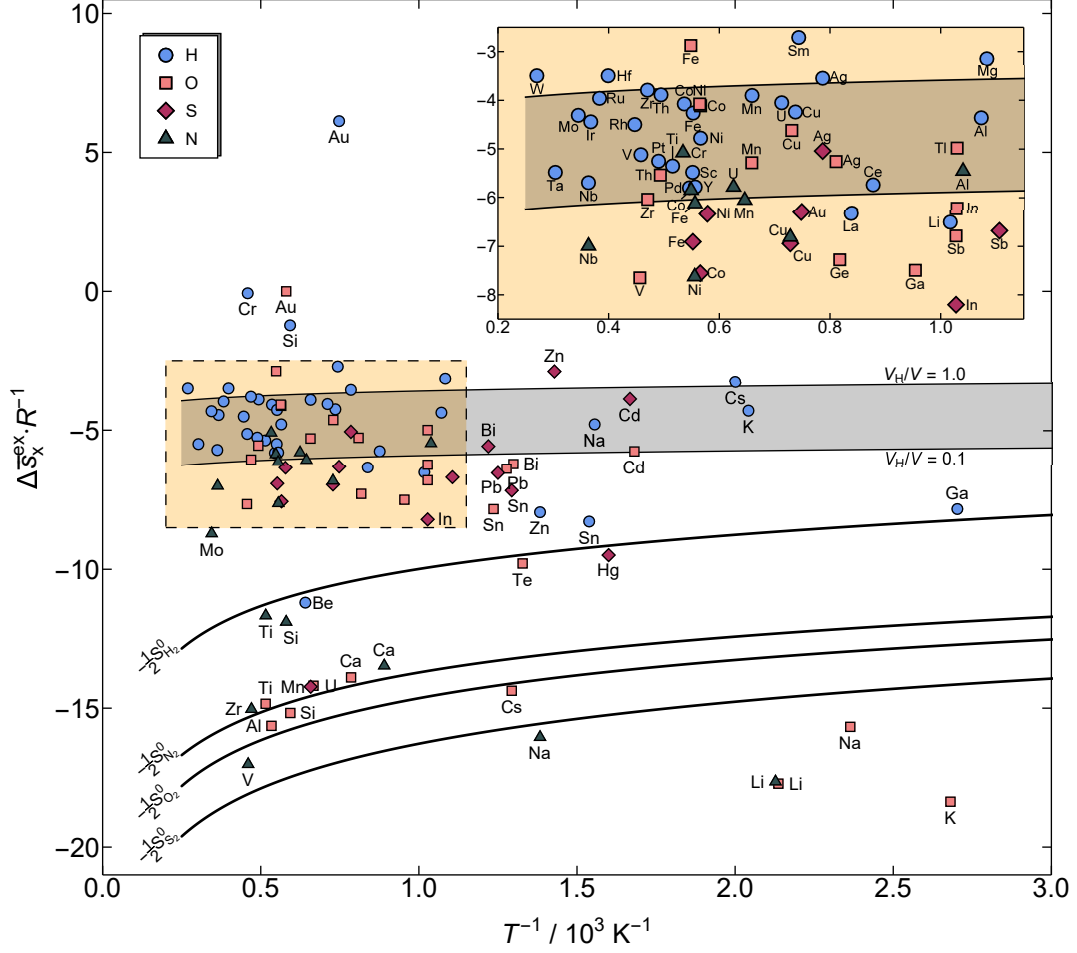


Figure 2: Partial molar entropy of mixing ($\Delta \bar{s}_X^{\text{ex}}$) as a function of $1/T$ for X: H (●), O (■), S (◆), N (▲) in liquid metals. The shaded band is the theoretical $\Delta \bar{s}_H^{\text{ex}}$ (Eq. 18) derived from the proton gas model [6] for values of V_H/V between 0.1 (lower curve) and 1.0 (upper curve). The majority of the data for the M-H systems lie within this range of theoretical entropy values. The solid curves are $\frac{1}{2} s_{X_2}^0$, the standard state entropy of dissolved X, as functions of temperature. The inset plot shows the boxed and shaded region in the full figure.

214 V_H , the classical configuration integral, has a definite physical meaning that can
 215 be understood within the context of short range order in the M-H system. An
 216 immediate consequence of this view is that the shift in $\Delta \bar{s}_H^{\text{ex}}$ across the solid-
 217 liquid transition is the result of the local structural changes that occur during
 218 melting. This is the same conclusion proposed in Section 2 from a heuristic

219 argument about chemical interaction energies, which can now be more rigorously
 220 treated using the proton gas model.

221 The connection to short range order may be made recalling first that W is
 222 the potential energy of the H assembly above its ground state energy in the
 223 metal. W is a function of the spatial coordinates of the H atoms. In the limit
 224 that $W \rightarrow 0$ everywhere in the metal, $V_H = V$. As W increases, $V_H < V$, and the
 225 effective volume in which H is well-described as a proton gas decreases. Stated
 226 differently, the tendency for M-H compound formation increases. V_H , then, is
 227 a quantity that reflects the strength of the association between H and metal
 228 atoms. Second, the interpretation of V_H as a measure of short range ordering
 229 requires a formal connection to the local M-H interactions. As of yet in this
 230 analysis, no description of the *distribution* of V_H over the volume of the metal
 231 has been provided. Fowler [6] makes the connection between the proton gas
 232 occupying an effective volume V_H and the short-range interaction between M
 233 and H by showing that, in the limit of small H solubility ($N_H \ll \alpha N_M$, where α
 234 is the number of H coordination sites per metal atom), it is valid to describe each
 235 H atom as being bound to a potential field of volume $v'_H = V_H/(\alpha N_M)$, where α
 236 is the number of H coordination sites per metal atom. Thus, one may interpret
 237 V_H as being uniformly distributed over αN_M interstitial (or quasi-interstitial)
 238 sites, each with a volume v'_H , associated with the metal atoms. The connection
 239 with short range order is now immediately clear. As W increases, reflecting
 240 a greater propensity for M-H compound formation, the effective volume v'_H in
 241 which each H atom freely translates decreases.⁴ A localization of the H atoms
 242 with respect to the metal atoms is found and hence an increase in the short range
 243 order of the M-H system. The loss of entropy corresponding to an increase in
 244 W is appropriately reflected in Eq. 18, where, as V_H decreases, $\Delta \bar{s}_H^{\text{ex}}$ decreases.

245 From Eqs. 5 and 18, the change in $\Delta \bar{s}_H^{\text{ex}}$ across the solid-liquid transition,
 246 $\Delta \Delta \bar{s}_H^{\text{ex}}$, may be written as:

⁴The H partition function in the proton gas model is classical. By treating H as a particle in an infinite potential well, one can show that for v'_H less than approximately 10^{-3} nm^3 , recourse must be made to quantum statistical mechanics, as the difference between the energy states of H is no longer much less than kT .

$$\Delta\Delta\bar{s}_H^{\text{ex}} = R \ln \left(\frac{V_{H,\text{liq}}}{V_{H,\text{sol}}} \right) \quad (19)$$

where the entropy is per mole of H rather than per atom. The value of $V_{H,\text{sol}}$ for most metals for temperatures on the order of 10^3 K varies from about 0.1 to 1.0 and is typically less than 0.5 for transition metals [40]. The magnitude of $\Delta\Delta\bar{s}_H^{\text{ex}}$ is then bounded by making use of the following arguments: $V_H \leq V$ and $V_{H,\text{liq}}/V_{H,\text{sol}} > 1$, the latter inequality being a consequence of the expectation that the liquid is a more disordered state than the solid ($W_{\text{liq}} < W_{\text{sol}}$). This yields a range of possible values for $\Delta\Delta\bar{s}_H^{\text{ex}}$:

$$R \ln(1) < \Delta\Delta\bar{s}_H^{\text{ex}} \leq R \ln(10). \quad (20)$$

The lower and upper bounds are 0 and $2.3R$, respectively. This range adequately accounts for the measured values of $\Delta\Delta\bar{s}_H^{\text{ex}}$ shown in Fig. 1, the average value of which is $1.3R$.

The change in $\Delta\bar{h}_H^{\text{mix}}$ at the solid-liquid transition, $\Delta\Delta\bar{h}_H^{\text{mix}}$, follows directly from Eqs. 4 and 17:

$$\Delta\Delta\bar{h}_H^{\text{mix}} = \Delta\chi_s \quad (21)$$

where $\Delta\chi_s$ is the difference between the H ground state energy (“absorption” enthalpy) in the liquid and solid states. Further discussion of Eq. 21 is limited, as the value of χ_s cannot be determined from the proton gas model. Other theoretical approaches are needed to rationalize the connection, if it exists, between Eq. 21 and the average measured value of $\Delta\Delta\bar{h}_H^{\text{mix}}$ of $1000R$ J mol⁻¹ H. It is for this reason that the present discussion primarily concerns the partial molar entropy.

A connection has been made between short range order and $\Delta\bar{s}_H^{\text{ex}}$. Specifically, the change in $\Delta\bar{s}_H^{\text{ex}}$ at T_{fus} , $\Delta\Delta\bar{s}_H^{\text{ex}}$, can be seen as the result of changes in short range order across melting (Eq. 20). The most direct means of experimentally validating such a connection would be neutron diffraction measurements of several of the metals in Table 1 above and below T_{fus} and at concentrations of dissolved H where Eq. 3 is true. Currently, the local structure is known only for select solid state M-H systems at relatively low temperatures [20]. Comparatively more is known about the structure of *pure* liquid metals, and some

insight may be found by examining the changes in short range order that occur at the solid-liquid transition of the metal solvent. First, it is well-known that the molar volume increases between 2–5 % for most metals upon melting [39, 41]. In addition, small changes in coordination number have been inferred from X-ray and neutron diffraction measurements of a number of solid and liquid metals [42]. The change in coordination number at melting is crystal-dependent: approximately -1 for close-packed metals and $+2$ to $+3$ for BCC metals. Lastly, one may infer information about the short range order in metals from band structure-dependent electronic properties [43]. Both nuclear magnetic resonance measurements [44] and photoelectron spectroscopy [45] suggest measurable, but small, differences in short range order between the solid and liquid, which largely corroborate the diffraction studies. From the above points, it is clear some change in short range order of the metal does occur at melting, though the change is not large. The increase in molar volume and changes in the M-M coordination number leave open the possibility of an increase in the number of H sites at melting, which would yield the relation $\Delta\Delta\bar{s}_H^{\text{ex}} > 0$ implied in Eq. 20. It must be stressed that the relevant ordering in this analysis is that between the metal and dissolved H. Information about M-M short range order, such as coordination number and nearest-neighbor distance, is, on its own, insufficient to corroborate Eq. 20.

5. Conclusion

A systematic change in $\Delta\bar{h}_H^{\text{mix}}$ and $\Delta\bar{s}_H^{\text{ex}}$ of approximately $1000R$ and $1.3R$, respectively, occurs at the solid-liquid transition for a number of M-H systems in the dilute limit. To rationalize these changes from first-principles, expressions for $\Delta\bar{h}_H^{\text{mix}}$ and $\Delta\bar{s}_H^{\text{ex}}$ were derived from the proton gas model of Fowler and Smithells [6]. Good agreement was observed between the theoretical and experimental values of $\Delta\bar{s}_H^{\text{ex}}$ for values of the classical configuration integral (V_H) between 0.1 and 1.0. The change in $\Delta\bar{s}_H^{\text{ex}}$ at melting, $\Delta\Delta\bar{s}_H^{\text{ex}}$, is directly related to the change in V_H , from which the following bounds were derived: $R\ln(1) < \Delta\Delta\bar{s}_H^{\text{ex}} \leq R\ln(10)$. This range of 0–2.3 R reflects the range of measured values for $\Delta\Delta\bar{s}_H^{\text{ex}}$, the average being 1.3 R . It was proposed that V_H is a quantity which reflects short range order in the M-H system. Consequently,

the measured values of $\Delta\Delta\bar{s}_H^{\text{ex}}$ correspond to a decrease in short range order at melting. Qualitatively, the notion that H short range order decreases in the liquid state is supported by investigations of structural changes in pure liquid metals. The statistical mechanical description of H dissolved in liquid metals remains a frontier for thermodynamicists. Considering the importance of H control in process metallurgy, further studies of this topic are of significant practical interest.

6. Acknowledgments

This work was supported by the National Science Foundation (NSF) under grant number 1562545.

Appendix A. The Grand Canonical Partition Function

The general form of the grand canonical partition function of the proton gas model of H solubility is:

$$\Gamma = \sum_{N_H} Q(N_H, V, T) e^{N_H \mu_H / kT} e^{-N_H \chi_s / kT}. \quad (\text{A.1})$$

Upon expanding terms, Γ may be written as:

$$\begin{aligned} \Gamma &= \sum_{N_H} [\Omega_H(T) \times \phi_H(T)^{N_H}] e^{N_H \mu_H / kT} e^{-N_H \chi_s / kT} \\ &= \sum_{N_H} \left[\left(\frac{1}{N_H!} \int \cdots \int e^{-W/kT} \prod_{i=1}^{N_H} (dx dy dz)_i \right) \times \left(\frac{2\pi m_H kT}{h^2} \right)^{3N_H/2} \omega^{N_H} \right] e^{N_H \mu_H / kT} e^{-N_H \chi_s / kT} \\ &= \sum_{N_H} \frac{1}{N_H!} \left[\int_V e^{-W/kT} dV \times \left(\frac{2\pi m_H kT}{h^2} \right)^{3/2} \omega \lambda_H(T) \right]^{N_H} e^{-N_H \chi_s / kT} \\ &= \exp \left(l_H \lambda_H \omega e^{-\chi_s / kT} \right). \end{aligned} \quad (\text{A.2})$$

$\Omega_H(T)$ is the configurational potential energy partition function. $\phi_H(T)$ is the molecular partition function of the dissolved H without the volumetric factor. μ_H is the chemical potential of H.

323 Appendix B. Entropy and Enthalpy of Hydrogen Gas

324 The absolute activity of atomic hydrogen gas is [40]:

$$\lambda_g = \left(\frac{P}{kT}\right)^{\frac{1}{2}} e^{\frac{-\chi_d}{kT}} \left[\left(\frac{4\pi m_H kT}{h^2}\right)^{\frac{3}{2}} \frac{8\pi^2 A kT \omega^2}{2h^2} \right]^{-\frac{1}{2}}. \quad (\text{B.1})$$

325 The same approach for deriving the total partial molar entropy of dis-
326 solved H may be applied here to determine the molar entropy of H gas, s_g .

$$\begin{aligned} s_g &= - \left(\frac{\partial \mu_g}{\partial T} \right)_P \\ &= - \frac{\partial}{\partial T} kT \ln \lambda_g \Big|_P \\ &= k \left(\frac{7}{4} - \frac{1}{2} \ln \left(\frac{P}{k} \right) + \frac{7}{4} \ln T + \frac{3}{4} \ln \left(\frac{4\pi m_H k}{h^2} \right) + \frac{1}{2} \ln \left(\frac{8\pi^2 A k}{h^2} \right) + \frac{1}{2} \ln \left(\frac{\omega^2}{2} \right) \right) \end{aligned} \quad (\text{B.2})$$

327 The molar enthalpy of H gas, h_g , is

$$\begin{aligned} h_g &= \left(\frac{\partial \mu_g / T}{\partial (1/T)} \right)_P \\ &= - \frac{\partial}{\partial (1/T)} kT \ln \lambda_g \Big|_P \\ &= k \left(\frac{7}{4} T - \frac{\chi_d}{2k} \right). \end{aligned} \quad (\text{B.3})$$

List of Symbols

A	Moment of inertia of $\text{H}_{2(\text{g})}$ (4.63×10^{-34} kg m ²)
a_{H}	Activity of H
h	Planck constant (6.626×10^{-34} J s)
$\Delta \bar{h}_i^{\text{mix}}$	Relative partial molar enthalpy of mixing (J mol ⁻¹)
	Difference between $\Delta \bar{h}_{i,\text{liq}}^{\text{mix}}$ and $\Delta \bar{h}_{i,\text{sol}}^{\text{mix}}$ at T_{fus}
$\Delta \Delta \bar{h}_i^{\text{mix}}$	(J mol ⁻¹)
k	Boltzmann constant (1.38×10^{-23} J K ⁻¹)
l_{H}	Molecular translational partition function of H
M_{M}	Molecular weight of M (kg mol ⁻¹)
m_{H}	Mass of H (1.69×10^{-27} kg)
N_A	Avogadro constant (6.022×10^{23} mol ⁻¹)

Continued on next page

N_H	Equilibrium number of dissolved H
N_M	Number of M atoms
n_i	Number of moles of i
P_i	Absolute pressure of i (Pa)
p_i	Partial pressure of i
Q	Canonical partition function
q_H	Molecular partition function of dissolved H
R	Gas constant (8.314 J K ⁻¹ mol ⁻¹)
r_i	Ratio of $x_{i,\text{liq}}$ to $x_{i,\text{sol}}$
s_i^0	Standard state molar entropy (J K ⁻¹ mol ⁻¹)
\bar{s}_i	Partial molar entropy (J K ⁻¹ mol ⁻¹)
$\Delta \bar{s}_i^{\text{ex}}$	Relative partial molar excess entropy (J K ⁻¹ mol ⁻¹)
$\Delta \Delta \bar{s}_i^{\text{ex}}$	Difference between $\Delta \bar{s}_{i,\text{liq}}^{\text{ex}}$ and $\Delta \bar{s}_{i,\text{sol}}^{\text{ex}}$ (J K ⁻¹ mol ⁻¹)
T	Temperature (K)
T_{fus}	Melting temperature (K)
V	Volume (m ³)
V_H	Classical configuration integral (m ³)
W	Configurational potential energy of the M-H assembly (J)
x_i	Mole fraction of i
y_i	Mole ratio of i
z_i	Lattice ratio of i
z'_i	Occupied-unoccupied site ratio: $z'_i = z_i/\alpha$
Greek	
α	Number of H coordination sites per atom of M
Γ	Grand canonical partition function of dissolved H
γ_i	Activity coefficient of i
λ_H	Absolute activity of H
μ_H	Chemical potential of H (J mol ⁻¹)
ρ_M	Density of M (kg m ⁻³)
ϕ_H	Molecular partition function of H without the volumetric factor (m ⁻³)
χ_d	Dissociation energy of diatomic H _{2(g)} (J)
χ_s	Ground state energy of dissolved H (J)
Ω_H	Configurational potential energy partition function
ω	H nuclear spin statistical weight

328 References

- 329 [1] J. P. Hirth, Effects of hydrogen on the properties of iron and steel, Metal-
330 lurgical Transactions A 11 (6) (1980) 861–890.
- 331 [2] A. R. Troiano, The role of hydrogen and other interstitials in the mechanical
332 behavior of metals, Transactions of the American Society for Metals 52
333 (1960) 54–80.
- 334 [3] Y. A. Chang, K. Fitzner, M. X. Zhang, The solubility of gases in liquid
335 metals and alloys, Progress in Materials Science 32 (2-3) (1988) 97–259.
- 336 [4] E. Fromm, E. Gebhardt, Gase und Kohlenstoff in Metallen, Springer-
337 Verlag, Berlin; New York, 1976.
- 338 [5] F. D. Manchester (Ed.), Phase Diagrams of Binary Hydrogen Alloys, ASM
339 International, Materials Park, OH, 2000.
- 340 [6] R. H. Fowler, C. J. Smithells, A theoretical formula for the solubility of
341 hydrogen in metals, Proceedings of the Royal Society A: Mathematical,
342 Physical and Engineering Sciences 160 (900) (1937) 37–47.
- 343 [7] Y. Ebisuzaki, M. O’Keeffe, The solubility of hydrogen in transition metals
344 and alloys, Progress in Solid State Chemistry 4 (1967) 187–211.
- 345 [8] T. Emi, R. D. Pehlke, Theoretical calculation of the solubility of hydrogen
346 in liquid metals, Metallurgical Transactions 1 (10) (1970) 2733–2737.
- 347 [9] M. O’Keeffe, S. A. Steward, Analysis of the thermodynamic behavior
348 of hydrogen in body-centered-cubic metals with application to niobium-
349 hydrogen, Berichte Der Bunsen-gesellschaft Fur Physikalische Chemie
350 76 (12) (1972) 1278–1282.
- 351 [10] S. Stafford, R. B. McLellan, The solubility of hydrogen in nickel and cobalt,
352 Acta Metallurgica 22 (12) (1974) 1463–1468.
- 353 [11] O. J. Kleppa, P. Dantzer, M. E. Melnichak, High-temperature thermody-
354 namics of the solid solutions of hydrogen in bcc vanadium, niobium, and
355 tantalum, Journal of Chemical Physics 61 (10) (1974) 4048–4058.

- [12] A. Magerl, N. Stump, H. Wipf, G. Alefeld, Interstitial position of hydrogen in metals from entropy of solution, *Journal of Physics and Chemistry of Solids* 38 (7) (1977) 683–686.
- [13] P. G. Dantzer, O. J. Kleppa, High-Temperature Thermodynamics of Dilute Solutions of Hydrogen and Deuterium in Tantalum and in Tantalum-Oxygen Solid Solutions, *Journal of Solid State Chemistry* 24 (1978) 1–9.
- [14] A. Mainwood, A. M. Stoneham, The theory of the entropy and enthalpy of solution of chemical impurities: I. General method, *Philosophical Magazine B* 37 (2) (1978) 255–261.
- [15] G. Boureau, O. J. Kleppa, P. D. Antoniou, Thermodynamic Aspects of Hydrogen Motions in Dilute Metallic Solutions, *Journal of Solid State Chemistry* 28 (1979) 223–233.
- [16] P. Dantzer, O. Kleppa, Thermodynamics of the Lanthanum-Hydrogen System at 917K, *Journal of Solid State Chemistry* 35 (1980) 34–42.
- [17] S. Yamanaka, Y. Fujita, M. Uno, M. Katsura, Influence of interstitial oxygen on hydrogen solubility in metals, *Journal of Alloys and Compounds* 293 (1999) 42–51.
- [18] A. Sieverts, Absorption of gases by metals, *Zeitschrift für Metallkunde* 21 (1929) 37–46.
- [19] S. A. Gedeon, T. W. Eagar, Thermochemical analysis of hydrogen absorption in welding, *Welding Journal* 69 (7) (1990) 264–271.
- [20] Y. Fukai, *The Metal-Hydrogen System: Basic Bulk Properties*, 2nd Edition, Springer-Verlag, Berlin, Heidelberg, 2005.
- [21] P. R. Subramanian, Ag-H (Silver-Hydrogen), in: F. D. Manchester (Ed.), *Phase Diagrams of Binary Hydrogen Alloys*, ASM International, Materials Park, OH, 2000, pp. 1–3.
- [22] E. Fromm, G. Horz, Hydrogen, nitrogen, oxygen, and carbon in metals, *International Metals Reviews* 25 (1) (1980) 269–311.

- 384 [23] F. D. Manchester, A. San-Martin, Al-H (Aluminum-Hydrogen), in: F. D.
385 Manchester (Ed.), Phase Diagrams of Binary Hydrogen Alloys, ASM In-
386 ternational, Materials Park, OH, 2000, pp. 4–12.
- 387 [24] P. N. Anyalebechi, Analysis and thermodynamic prediction of hydrogen
388 solubility in solid and liquid multicomponent aluminum alloys, in: B. Welch
389 (Ed.), Light Metals 1998, Minerals, Metals and Materials Society, 1998, pp.
390 185–200.
- 391 [25] M. Weinstein, J. F. Elliott, The Solubility of Hydrogen in Liquid Pure
392 Metals Co, Cr, Cu, and Ni, Transactions of the Metallurgical Society of
393 AIME 227 (1) (1963) 285–286.
- 394 [26] V. I. Shapovalov, Hydrogen as an alloying element in metals, Russian Jour-
395 nal of Physical Chemistry A 54 (11) (1980) 1659–1663.
- 396 [27] A. San-Martin, F. D. Manchester, The Fe-H (Iron-Hydrogen) System, Bul-
397 letin of Alloy Phase Diagrams 11 (2) (1990) 173–184.
- 398 [28] F. D. Manchester, A. San-Martin, H-Mg (Hydrogen-Magnesium), in: F. D.
399 Manchester (Ed.), Phase Diagrams of Binary Hydrogen Alloys, ASM In-
400 ternational, Materials Park, OH, 2000, pp. 83–94.
- 401 [29] A. Sieverts, H. Moritz, Manganese and hydrogen, Zeitschrift Fur Physikalis-
402 che Chemie-abteilung A-chemische Thermodynamik, Kinetik, Elektro-
403 chemie Eigenschaftslehre 180 (1937) 249–263.
- 404 [30] A. San-Martin, F. D. Manchester, H-Mn (Hydrogen-Manganese), in: F. D.
405 Manchester (Ed.), Phase Diagrams of Binary Hydrogen Alloys, ASM In-
406 ternational, Materials Park, OH, 2000, pp. 95–104.
- 407 [31] J. A. Pryde, C. G. Titcomb, Phase equilibria and kinetics of evolution of
408 dilute solutions of hydrogen in niobium, Journal Of Physics C-Solid State
409 Physics 5 (12) (1972) 1293–1300.
- 410 [32] E. Veleckis, R. K. Edwards, Thermodynamic Properties in the Systems
411 Vanadium-Hydrogen, Niobium-Hydrogen, and Tantalum-Hydrogen, Jour-
412 nal of Physical Chemistry 7 (9) (1969) 683–692.

- [33] M. L. Wayman, G. C. Weatherly, H-Ni (Hydrogen-Nickel), in: F. D. Manchester (Ed.), Phase Diagrams of Binary Hydrogen Alloys, ASM International, Materials Park, OH, 2000, pp. 147–157.
- [34] N. N. Kalinyuk, Solubility of hydrogen in solid and in liquid palladium, Russian Journal of Physical Chemistry A 54 (1980) 1611–1613.
- [35] F. D. Manchester, A. San-Martin, H-Ti (Hydrogen-Titanium), in: F. D. Manchester (Ed.), Phase Diagrams of Binary Hydrogen Alloys, ASM International, Materials Park, OH, 2000, pp. 238–258.
- [36] P. Dantzer, High temperature thermodynamics of H₂ and D₂ in titanium, and in dilute titanium oxygen solid solutions, Journal of Physics and Chemistry of Solids 44 (9) (1983) 913–923.
- [37] C. H. P. Lupis, Chemical Thermodynamics of Materials, Prentice-Hall, Inc., New York, 1983.
- [38] F. D. Richardson, Physical Chemistry of Melts in Metallurgy, Academic Press Inc. Ltd., London, 1974.
- [39] O. Kubaschewski, The change of entropy, volume and binding state of the elements on melting, Transactions of the Faraday Society 45 (1949) 931–940.
- [40] R. Fowler, E. A. Guggenheim, Statistical Thermodynamics, Cambridge University Press, Cambridge, 1965.
- [41] G. Kaptay, A unified model for the cohesive enthalpy, critical temperature, surface tension and volume thermal expansion coefficient of liquid metals of bcc, fcc and hcp crystals, Materials Science and Engineering A 495 (1-2) (2008) 19–26.
- [42] Y. Waseda, The structure of liquid transition metals and their alloys, in: R. Evans, D. A. Greenwood (Eds.), Liquid Metals, 1976 (Institute of Physics Conference Series No. 30), The Institute of Physics, Bristol, 1977, pp. 230–240.
- [43] N. E. Cusack, The electronic properties of liquid metals, Reports on Progress in Physics 26 (1963) 361–409.

- 443 [44] W. Knight, A. Berger, V. Heine, Nuclear resonance in solid and liquid
444 metals: A comparison of electronic structures, *Annals of Physics* 8 (2)
445 (1959) 173–193.
- 446 [45] C. Norris, Photoelectron spectroscopy of liquid metals and alloys, in:
447 R. Evans, D. A. Greenwood (Eds.), *Liquid Metals*, 1976 (Institute of
448 Physics Conference Series No. 30), The Institute of Physics, Bristol, 1977,
449 pp. 171–180.